Mosaicing of Flattened Images from Straight Homogeneous Generalized Cylinders

Adrian G. Borş[1], William Puech[2],

Ioannis Pitas[1], and Jean-Marc Chassery[2]

[1] Department of Informatics, University of Thessaloniki, Box 451,
54006 Thessaloniki, Greece - {adrian,pitas}@zeus.csd.auth.gr
[2] TIMC-IMAG Laboratory, Institut Albert Bonniot, Domaine de la Merci,
38706 La Tronche Cedex, France - {William.Puech,Jean-Marc.Chassery}@imag.fr

Abstract. This paper presents a new method for reconstructing paintings from component images. A set of monocular images of a painting from a straight homogeneous generalized cylinder is taken from various viewpoints. After deriving the surface localization in the camera coordinate system, the images are backprojected on the curved surface and flattened. We derive the perspective distortion of the scene in the case when it is mapped on a cylindrical surface. Based on the result of this study we derive the necessary number of views in order to represent the entire scene depicted on a cylindrical surface. We propose a matching-based mosaicing algorithm for reconstructing the scene from the curved surface. The proposed algorithm is applyed on paintings.

1 Introduction

In this study we consider images taken by monocular vision. Let us consider a painting on a straight homogeneous generalized cylinder [1]. We identify the localization parameters of the painted surface by considering the projections of two parallels in the given image. We calculate the common normal of the parallels projections and we derive the localization parameters. Based on the localization parameters we backproject the image on the curved surface and afterwards we flatten it [2].

The difference in perspective distortion has been used for computing the shape of the curved surface from texture information [3]. In this paper we analyze the geometrical distortions caused by the perspective view in the case of images painted on cylindrical surfaces.

Mosaicing is a well known technique used for representing images of paintings [4, 5]. Distortions caused by the painting surface shape must be corrected before the mosaicing. In [6] the perspective projection distortions caused by rotating a camera around its focal point are corrected by projecting the images onto a Gaussian sphere which is flattened on a plane tangent to it. Mosaicing assemble a set of images, each representing details of a certain region of the painting, in order to reconstruct the entire scene. The methods used in [4, 6] employ the matching of manually selected points. In this study we propose an automatic

mosaicing method [7] based on region matching [5]. In the case when the images are obtained by flattening the representations of a curved surface, the image regions with large distortions, caused by perspective projection, are excluded from matching. We evaluate the bounds of the necessary number of views in order to represent the entire painting from a cylinder. The proposed method is applied in painting visualization and the result can be further used for painting restoration.

2 Curved Surface Localization and Flattening

In order to perform the localization from a single perspective view, we limit our study to the case when the surface has a curvature different than zero in only one direction. The localization is described by three rotation angles : θ_x, θ_y and θ_z. These rotation angles provide the relationship between the camera coordinate system and the coordinate system of the curved surface. Two projection axes must be localized [2]. First we find the projection of the revolution axis, and afterwards we derive the position of the second axis corresponding to the projection of one particular parallel. In order to find the projection of the revolution axis, we identify the common normal P_1P_2 of two parallel curves which are projected in the image, as shown in Figure 1 and described in [2]. The slope of the straight line P_1P_2 gives us the axis' direction. In the image coordinate system (u, v), the equation of this axis is :

$$v = A_1.u + B_1,\tag{1}$$

where A_1 and B_1 are the coefficients of the straight line P_1P_2. From the equation (1) we derive the rotation angle θ_z corresponding to the angle between u and the revolution axis, as shown in Figure 1:

$$\theta_z = \arctan(A_1).\tag{2}$$

Among all the parallels on the curved surface, only one is projected on the image as a straight line. This straight line belongs to the plane passing through that parallel and through viewpoint, and defines the second axis. In order to obtain the two other rotation angles, θ_x and θ_y, let us consider P, a point located on the curve passing through either P_1 or P_2. We define the curvature at a point P_i as :
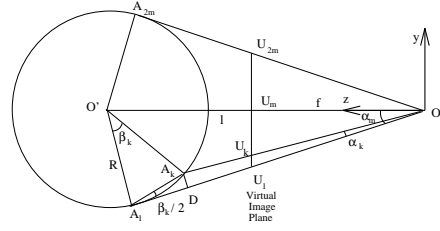
$$K_i = \lim_{P \to P_i} \frac{\alpha(P) - \alpha(P_i)}{|\widehat{PP_i}|},\tag{3}$$

where $i \in \{1, 2\}$, $\alpha(P_i)$ is the angle of the tangent to P_i, and $|\widehat{PP_i}|$ is the length of the arc between P and P_i. We denote by P_0, the point belonging to the revolution axis, where the curvature K_0 equals zero. Considering (u'_0, v'_0) the coordinates of P_0 we obtain the equation of the second axis :

$$v = -\frac{1}{A_1}.u + \left(v'_0 + \frac{u'_0}{A_1}\right).\tag{4}$$
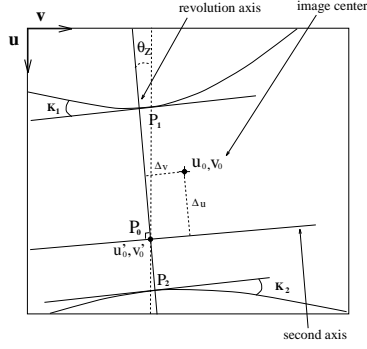
Figure 1. The two axes derived from parallel curves.

Figure 2. The cross-section representation through cylinder and image.

We denote by (Δ_u, Δ_v) the vector distance between (u_0, v_0) and P_0, the intersection of the two axes, as shown in Figure 2. The two rotation angles are then given by :

$$\begin{cases} \theta_x = \arctan(\frac{\Delta_v}{f.k}) \\ \theta_y = \arctan(\frac{\Delta_u}{f.k}), \end{cases} \tag{5}$$

where f is the focal distance and k is the resolution factor. Based on the localization parameters we backproject the image on the 3D surface, we match the point P_0 with the image center (u_0, v_0) and we obtain the virtual image. In the virtual image, P_0 is projected to the image center and the projection of the revolution axis is vertical. After backprojecting the image onto the curved surface, we flatten it in order to obtain a new image without geometrical distortions caused by the surface curvature [2, 7].

3 The Perspective Distortion Analysis when the Image is Backprojected on a Cylindrical Surface

The flattening method described in the previous Section recovers the distortions caused by the geometry of the painted surface, but not the distortions caused by perspective projection. Let us consider the image of a cylindrical surface constructed such that the axes of the camera coordinate system coincide with the object axes. The focal axis z is perpendicular to the revolution axis of the cylinder. The radius of the cylinder is denoted by R, and the viewpoint O is situated at a distance l from the revolution axis of the cylinder, as shown in the cross-section representation from Figure 2. The projection of the arc $|\widehat{A_1 A_{2m}}|$ to the virtual image plane is the line segment $|U_1 U_{2m}|$. The horizontal cross-section through image is discretized in $2m$ equal-sized intervals :

$$|U_k U_{k-1}| = |U_{k-1} U_{k-2}| = 1 \, \text{pixel for } k = 3, \ldots, 2m. \tag{6}$$
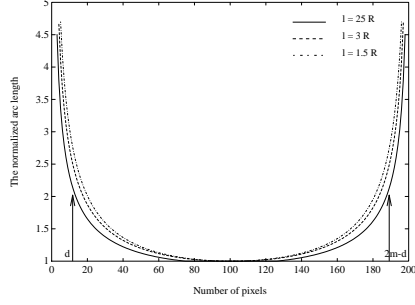
Figure 3. The length of the arcs each of them corresponding to an equal-sized image segment.
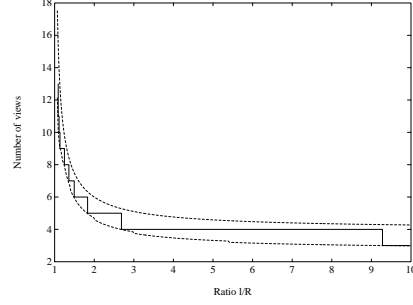
Figure 4. The necessary number of views.

Let us denote the angles $A_1\widehat{O}A_k$, $A_1\widehat{O'}A_k$ by α_k and β_k. Based on geometrical considerations, we express the length of the line segment $|A_kD|$ in Figure 2, in two different ways. From the triangles $O'A_1A_k$ and A_1A_kD we derive :

$$|A_kD| = 2R\sin^2\left(\frac{\beta_k}{2}\right). \tag{7}$$

$|A_kD|$ is calculated from the triangle A_kDO :

$$|A_kD| = (\sqrt{l^2 - R^2} - R\sin(\beta_k))\tan(\alpha_k). \tag{8}$$

From the triangle OU_kU_m we have :

$$\tan(\alpha_m - \alpha_k) = \frac{|U_mU_k|}{|U_mO|} = \frac{|U_mU_k|}{|U_1U_m|}\frac{|U_1U_m|}{|U_mO|} \tag{9}$$

Based on classical geometry properties in triangles OU_1U_m, $OO'A_1$ and by using (6) we find :

$$\tan(\alpha_m - \alpha_k) = \frac{m - k}{m}\frac{|O'A_1|}{|A_1O|} = \frac{m - k}{m\sqrt{\mu^2 - 1}} \tag{10}$$

where we denote $\mu = \frac{l}{R}$ and the angle $O'\widehat{O}A_1$ by α_m. Afterwards, we derive $\tan(\alpha_k)$ with respect to the number of pixels k :

$$\tan(\alpha_k) = \frac{k\sqrt{\mu^2 - 1}}{m\mu^2 - k}. \tag{11}$$

From (7), (8), and (11), we obtain :

$$2\sin^2\left(\frac{\beta_k}{2}\right) = (\sqrt{\mu^2 - 1} - \sin(\beta_k))\frac{k\sqrt{\mu^2 - 1}}{m\mu^2 - k} \tag{12}$$

for $k = 1, \ldots, 2m$. After deriving the angles β_k from (12), we compute the arc of the cylinder corresponding to an image segment of constant size :

$$|\widehat{A_kA_{k-1}}| = (\beta_k - \beta_{k-1})R. \tag{13}$$

The normalized arc length $|\widehat{A_kA_{k-1}}|$ / $|\widehat{A_mA_{m-1}}|$, calculated from (13) is represented in Figure 3 for $m = 100$, when $\mu \in \{1.5; 3; 25\}$. From this plot we observe that arcs of different length from the cylindrical surface are projected to segments with the same length in the image plane.

4   The Estimation of the Necessary Number of Views

Let us consider a set of images all taken at the same distance l from the cylinder's axis, each two neighboring images having an overlapping region. The region from the cylindrical surface which projects in the image without significant distortion contains neighboring arcs having small size variation from each other :

$$\left|\frac{|\widehat{A_k A_{k-1}}| - |\widehat{A_{k-1} A_{k-2}}|}{|\widehat{A_m A_{m-1}}| - |\widehat{A_{m-1} A_{m-2}}|}\right| = \left|\frac{\beta_k + \beta_{k-2} - 2\beta_{k-1}}{\beta_m + \beta_{m-2} - 2\beta_{m-1}}\right| \leq \delta \qquad (14)$$

where $|\widehat{A_k A_{k-1}}|$ and $|\widehat{A_{k-1} A_{k-2}}|$ are evaluated in (13), and δ is a small constant, measuring the difference in the arc length variation, representing a distortion measure.

As it can be observed from Figure 3, the neighboring images are likely to be differently distorted in the overlapping regions. The regions located towards the margins of the cylindrical surface representation are likely to contain larger distortions than the regions situated near the cylinder's axis projection. Let us consider that the minimal distortion condition from (14) is verified for $k = d, \ldots, 2m - d$, where d is the pixel index for which we obtain the equality in (14).

Each two images must overlap on a region corresponding to an angle larger than $2\beta_d$, i.e. where the distortions according to (14) are small enough. If we consider that each pixel in the scene should be projected in two neighboring images at most, we obtain the maximum number of images. The minimal and the maximal numbers of images required to represent the entire scene are :

$$\frac{\pi}{\arccos\left(\frac{R}{l}\right) - \beta_d} < n < \frac{2\pi}{\arccos\left(\frac{R}{l}\right)} \qquad (15)$$

where the angle β_d is derived from (14) and corresponds to the arc $|\widehat{A_1 A_d}|$. The bounds on the number of images to be taken around a cylinder are represented in Figure 4. In the same figure, the ceiling integer value of the minimum necessary number of views is marked by a continuous line. As we observe from this figure, the necessary number of images is large when the distance l from the viewpoint to the cylinders axis is small and decreases at three when is large.

5   The Mosaicing Algorithm

Image mosaicing is employed for assembling a set of images in order to reconstruct an entire scene [5]. The mosaicing approach proposed in this paper is based on matching [5, 7]. Only the part of the overlapping region which contains a small level of distortion, as provided by (14) is considered by the matching algorithm. Let us denote by (du, dv), the displacement between two neighboring images.

(a) Set of images to be mosaiced.   (b) The resulting image.

Figure 5. Mosaicing a set of infrared images in order to reconstruct a painting.

As in the case of the block matching algorithms [5] we define a search area $S_u \times S_v$ in the plane uOv. The overlapping part is found based on a search for the best matching between various regions from the two images in the given area :

$$(du, dv) = \arg \min_{k=1, l=1}^{S_u, S_v} \left(\sum_{i=2n-k}^{2n} \sum_{j=l}^{2m-2d} |\text{pel}_p(i - 2n + k, j - l) - \text{pel}_{p-1}(i, j)|, \right.$$

$$\left. \sum_{i=2n-k}^{2n} \sum_{j=l}^{2m-2d} |pel_p(i - 2n + k, j) - pel_{p-1}(i, j - l)| \right), \quad (16)$$

where $\text{pel}_p(i, j)$, $\text{pel}_{p-1}(i, j)$ are two pixel elements from two successive images $p - 1$, p, $(2m - 2d) \times 2n$ is the image size after eliminating the part containing distortions, and d is calculated according to (14).

To calculate the pixel values in the overlapping region we evaluate the minimum distance from a given pixel site (i, j) to the border of the common reliable image region :

$$g_{p-1} = \min\{i, j\} \ , \ g_p = \min\{dx - i, dy - j\} \quad (17)$$

for $i = 1, \ldots, du$ and $j = 1, \ldots, dv$. In order to ensure a smooth transition, the overlapping area pixels are taken as a weighting of the component images pixels with respect to the distance from the closest nonoverlapping region :

$$f(i, j) = \frac{g_p}{g_p + g_{p-1}} f_p(i, j) + \frac{g_{p-1}}{g_p + g_{p-1}} f_{p-1}(i, j), \quad (18)$$

where $f(i, j)$ and $f_p(i, j)$ denote a pixel element from the mosaiced image and from the pth image, respectively. The proposed procedure can be easily extended to mosaic many images having horizontal and vertical overlapping areas as exemplified on a set of infrared images of an old painting in Figure 5.

(a), (b) Original images of a painted arch ;
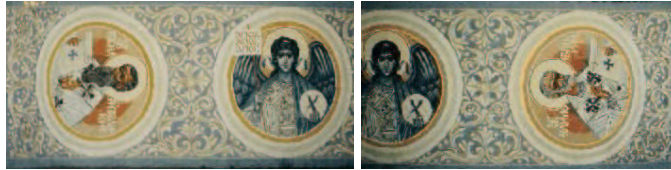
(c), (d) The flattened surface representations ;

(e) Result of the mosaicing algorithm ;

Figure 6. Reconstruction of an arch painting by mosaicing.

(a), (b), (c) Original images of a cup ;

(d), (e), (f) The flattened surface representations ;

(g) Result of the mosaicing algorithm ;

Figure 7. Reconstruction of the ceramic decorative pattern by mosaicing.

6 Simulation Results

The proposed algorithm was applied for reconstructing several paintings on convex, concave, or flat surfaces. In Figures 6 (a) and (b) two images representing parts of a Byzantine painting on an arch are shown. The algorithm was applied on the images of a cup represented in Figures 7 (a), (b), (c), as well. These images correspond to a parameter $\mu = l/R = 5.5$. From Figure 4 we observe that we need four images to represent the cup's surface. Due to the cup's handle and because the scene does not cover all around the cup, we use three images. These images present distortions, caused by the painted surface, that depend on the view-angle. We localize the painted surfaces by considering the projections of two parallels representing the edges of the arch or those of the decorative pattern from the cup. After finding the localization of the painted surface, we flatten the projected images of the paintings as shown in Figures 6 (c), (d) and 7 (d), (e), (f), respectively. The mosaicing of flattened representations are displayed in Figures 6 (e) and 7 (g). In color images, the localization parameters and the relative displacements of the images are calculated from the luminance component images. Afterwards, the result is applied on all the color components.

7 Conclusions

In this study we propose a new approach for representing the scenes painted on the surface of straight homogeneous generalized cylinders. We provide a theoretical analysis of the geometrical distortions due to the perspective projection and we derive the necessary number of views to represent entirely the scene painted on a cylindrical surface. We propose a new approach for image mosaicing based on matching. This algorithm is applied for painting visualization.

References

1. J. Ponce, D. Chelberg, W. B. Mann, "Invariant Properties of Straight Homogeneous Generalized Cylinders and their Contours," *IEEE Trans. on PAMI,* vol. 11, no. 9, pp. 951-966, 1989.
2. W. Puech, J.-M. Chassery, I. Pitas, "Curved surface localization in monocular vision," *Pattern Recognition Letters,* 1997 (to appear).
3. B. J. Super, A. C. Bovik, "Shape from texture using local spectral moments," *IEEE Trans. on PAMI,* vol. 17, no. 4, pp. 333-343, Apr. 1995.
4. R. J. Billinge, J. Cupitt, J, Dessipiris, D. Saunders, "A note on an Improved Procedure for the rapid assembly of infrared reflectogram mosaics," *Studies in Conservation,* vol. 38, pp. 92-97, 1993.
5. R. J. Schalkoff, *Digital Image Processing and Computer Vision.* John Wiley, 1989.
6. Ş. Gümüştekin, R. W. Hall, "Mosaic Image Generation on a Flattened Gaussian Sphere," *IEEE Workshop on Applications of Computer Vision,* Sarasota, USA, pp. 50-55, 1996.
7. W. Puech, A. G. Borş, J.-M. Chassery, I. Pitas, "Mosaicing of Paintings on Curved Surfaces," *IEEE Workshop on Applications of Computer Vision,* Sarasota, USA, pp. 44-49, 1996.